# Electroretinographic Abnormalities and Sex Differences Detected with Mesopic Adaptation in a Mouse Model of Schizophrenia: A and B Wave Analysis

Nathalia Torres Jimenez,[1–3] Justin W. Lines,[1,2] Rachel B. Kueppers,[3] Paulo Kofuji,[1,2] Henry Wei,[2] Amy Rankila,[2] Joseph T. Coyle,[4] Robert F. Miller,[1–3] and Linda K. McLoon[1–3]

[1]Graduate Program in Neuroscience, University of Minnesota, Minneapolis, Minnesota, United States
[2]Department of Neuroscience, University of Minnesota, Minneapolis, Minnesota, United States
[3]Department of Ophthalmology and Visual Neurosciences, University of Minnesota, Minneapolis, Minnesota, United States
[4]Department of Psychiatry, Harvard Medical School, Belmont, Massachusetts, United States

Correspondence: Linda K. McLoon, Department of Ophthalmology and Visual Neurosciences, University of Minnesota, Room 374 Lions Research Building, 2001 6th Street SE, Minneapolis, MN 55455, USA; mcloo001@umn.edu.

RFM and LKM are joint senior authors.
This study is part of the PhD thesis of Nathalia Torres Jimenez.

**Received:** January 3, 2019
**Accepted:** November 2, 2019
**Published:** February 13, 2020

Citation: Jimenez NT, Lines JW, Kueppers RB, et al. Electroretinographic abnormalities and sex differences detected with mesopic adaptation in a mouse model of schizophrenia: a and b wave analysis. *Invest Ophthalmol Vis Sci.* 2020;61(2):16. https://doi.org/10.1167/iovs.61.2.16

**Purpose.** Mesopic flash *electroretinography* (fERG) as a tool to identify *N*-methyl-D-aspartate receptor (NMDAR) hypofunction in subjects with schizophrenia shows great potential. We report the first fERG study in a genetic mouse model of schizophrenia characterized by NMDAR hypofunction from gene silencing of serine racemase (SR) expression ($SR^{-/-}$), an established risk gene for schizophrenia. We analyzed fERG parameters under various background light adaptations to determine the most significant variables to allow for early identification of people at risk for schizophrenia, prior to onset of psychosis. SR is a risk gene for schizophrenia, and negative and cognitive symptoms antedate the onset of psychosis that is required for diagnosis.

**Methods.** The scotopic, photopic, and mesopic fERGs were analyzed in male and female mice in both $SR^{-/-}$ and wild-type (WT) mice and also analyzed for sex differences. Amplitude and implicit time of the a- and b-wave components, b-/a-wave ratio, and Fourier transform analysis were analyzed.

**Results.** Mesopic a- and b-wave implicit times were significantly delayed, and b-wave amplitudes, b/a ratios, and Fourier transform were significantly decreased in the male $SR^{-/-}$ mice compared to WT, but not in female $SR^{-/-}$ mice. No significant differences were observed in photopic or scotopic fERGs between genotype.

**Conclusions.** The fERG prognostic capability may be improved by examination of background light adaptation, a larger array of light intensities, considering sex as a variable, and performing Fourier transform analyses of all waveforms. This should improve the ability to differentiate between controls and subjects with schizophrenia characterized by NMDAR hypofunction.

Keywords: electroretinogram, schizophrenia, NMDA receptor, biomarker, mice, a-wave, b-wave, mesopic

As part of the central nervous system, the retina has been considered to be the "window to the brain," as the retina and brain share many neurophysiological properties.[1] Thus, prior studies have demonstrated electroretinographic differences between subjects with schizophrenia and healthy controls.[2–7] These findings point toward visual deficits in individuals with schizophrenia not limited to higher level visual–cognitive processing but manifested at earlier stages of the visual pathway, including the retina. The significance of these findings focuses on the possibility of using retinal-evoked potentials as biomarkers for presymptomatic diagnosis of schizophrenia and for characterizing neurophysiologic abnormalities associated with schizophrenia or subgroups of schizophrenic subjects.[8–10] Although clinical interviews for the diagnosis of schizophrenia are effective at identifying schizophrenia once present, they have limited success in identifying presymptomatic individuals prior to the onset of psychosis.[11] Thus, an objective measurement prior to symptom onset would be invaluable for developing preventive interventions. Work by Hébert et al.[12] showed that young adult offspring of a parent with schizophrenia or bipolar disorder had reduced b-wave amplitudes; thus, in combination with the patient studies cited, these studies suggest that the retinal-evoked potential, the flash electroretinogram (fERG), may serve as a physiological metric for predicting schizophrenia in human subjects.

The fERG is a summed evoked potential from the retina in response to diffuse light. The advantage of the fERG as a diagnostic tool is that the technique is relatively noninvasive, easy to administer, and its major waves have known cellular origins.[13] The fERG response is well studied and has been recorded in many species, including humans and mice.[14] Despite clinical observations noting fERG abnormalities in individuals with schizophrenia, to date mouse

models of schizophrenia have not clearly defined what aspects of the fERG response might be most germane to use as a biomarker for schizophrenia or, specifically, a subtype associated with *N*-methyl-D-aspartic acid receptor (NMDAR) hypofunction. Identifying which of the fERG waves to use as a biometric measurement for a potential diagnosis of schizophrenia can be achieved more readily in mice because of greater control of parameters such as age, sex, treatment, and genetic status. There are now several excellent mouse models of schizophrenia to use for these analyses.

Proteomic and genomic analyses of synapses in human brain samples from controls or individuals with schizophrenia found altered expression of multiple proteins with known specific roles in NMDA function.[15,16] Although the proportion of individuals with schizophrenia in this subtype is not known, the NMDAR-related molecules are well represented in the identified risk genes.[15,16] The serine racemase (SR) gene is one of several risk genes for schizophrenia that affect NMDAR function and its downstream signaling.[17] Due to the importance of ensuring concordance between fERG abnormalities seen in individuals with schizophrenia and the mouse models with specific allelic variants similar to those seen in these individuals, we examined the fERGs from a schizophrenia mouse model, a serine racemase knockout ($SR^{-/-}$) that has been extensively evaluated for mimicking and studying chronic brain pathology in schizophrenia.[18] The $SR^{-/-}$ schizophrenia mouse model has a knockout of the gene for the enzyme SR and has reduced NMDAR function.[15]

The NMDAR is an ionotropic glutamate receptor that is critical for cellular communication and is found in both brain and retina. In the brain, the NMDAR receptor is critical for learning and memory. In the retina, NMDAR regulates light-evoked activity.[19–21] The hypothesized NMDAR relevance to schizophrenia originated after clinical observations of the recreational use of phencyclidine, which caused increased emergency room visits from patients exhibiting symptoms resembling schizophrenia.[22] This new hypothesis for NMDAR hypofunction as a potential etiology of schizophrenia is supported by pharmacological,[23,24] genetic,[25,26] clinical,[27,28] and postmortem studies[29–31] and provide evidence that NMDAR hypofunction is involved in the etiology of schizophrenia.[32] In our study, we have utilized an NMDAR hypofunction mouse model of schizophrenia ($SR^{-/-}$) to identify which of the fERG waves would best serve as a marker for NMDAR hypofunction. This mouse model for NMDAR hypofunction has a null mutation in the SR gene.[33] SR synthesizes D-serine, the primary co-agonist of NMDARs in forebrain[13] and the retina.[34] As a component of the central nervous system, the retina can acquire cellular abnormalities similar to those that are present in the brain.[9,35–38] Given that fERGs allow the evaluation of the functional integrity of the retina, they have the potential to become a useful non-invasive tool to assess pathological abnormalities in the brain.[9,39]

The fERG response is characterized by two low-frequency waves, the a- and b-waves, and high-frequency wave forms called oscillatory potentials (Fig. 1).[13,14] Both the a-wave and b-wave have known cellular origins.[13,14] The first wave in the fERG is the a-wave,[40–42] which is a corneal-negative potential that originates from photoreceptor activity.[40] The a-wave is followed by the b-wave, which is a corneal-positive potential originating from bipolar cells.[40,43–46] The b-wave response has been attributed to Müller glial cells. However, examination of mice where Müller cells were functionally inactivated resulted in no change in the b-wave, suggesting that they are not involved.[47] Riding on the ascending limb of the b-wave are the oscillatory potentials (OPs), which are hypothesized to originate from amacrine and retinal ganglion cells (RGCs).[40,44,48] It has been hypothesized that the OPs are due to dopaminergic inhibitory activity within amacrine cells and then generated by bipolar cells.[48] The clinical literature showed reduction in both the a- and b-waves in subjects with schizophrenia compared to controls; however, these studies did not fully address known gender and age differences associated with the fERG waveforms in human controls.[49–51] In healthy humans, longitudinal fERG studies demonstrated a linear decrease with age in the b-wave amplitude in men; females showed a linear decrease until ages 40 to 49 years, when there was a significant increase in the b-wave amplitude, speculated to be from hormonal changes.[50,51] Prior to age 40 in healthy females, b-wave amplitudes were significantly different from males. Not only were age and gender differences observed, but there is abundant literature on gender differences in people with schizophrenia, as well. For example, symptomatic onset of schizophrenia occurs later in females and is often less severe than in males.[52–54] These gender and age differences in people with schizophrenia could hypothetically be reflected in the fERGs, thus highlighting the importance of including age and gender in the fERG analyses.

Because age and gender differences can affect the fERG, we conducted in vivo fERG recordings, controlled for the mouse age, and analyzed sex differences; however, rather than use only light- or dark-adapted analyses based on International Society for Clinical Electrophysiology of Vision (ISCEV) standards,[55] we also adapted the mice under mesopic conditions. Previous studies showed that this method provides a good indicator of pathology in diabetic retinopathy[56,57] and schizophrenia.[2] The use of mesopic conditions allowed visualization of the differences in the a- and b-wave amplitudes in people with schizophrenia in comparison to controls. We recorded from young mice to evaluate whether a reduction in the functionality of the NMDAR results in any of the fERG abnormalities observed in people with schizophrenia. Additionally, we performed a second analysis of the resulting fERG waveforms to determine if sex-related differences were present.

## Methods

### Animals

Littermate male and female mice at 8 to 10 weeks of age from serine racemase null ($SR^{-/-}$) mutant mice developed as described by Basu et al.[18] and wild-type (WT) littermate controls were studied. In the first cohort, 34 mice were used under mesopic adaptation, 8 and 9 per genotype for males and females, respectively. We tested a second cohort of 30 mice, 8 $SR^{-/-}$ and 7 WT of each sex, under all three light conditions—light-, mesopic-, and dark-adapted—to ensure that we generated results similar to those for the first group of mice tested. All procedures followed the standards of the National Institutes of Health and the Association for Research in Vision and Ophthalmology Statement for the Use of Animals in Ophthalmic and Vision Research and were approved by the Institutional Animal Care and Use Committee at the University of Minnesota.

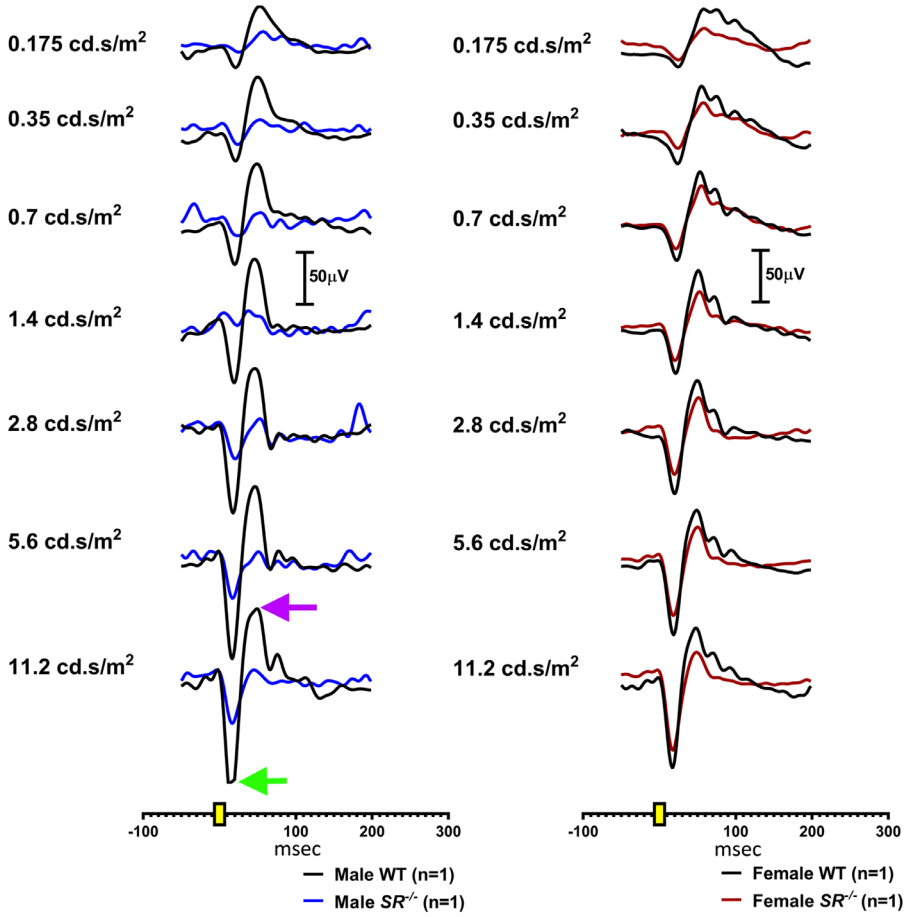


**Figure 1.** Representative filtered mesopic fERG recordings from WT mice (black), $SR^{-/-}$ male mice (blue), and $SR^{-/-}$ female mice (red) at seven light intensities at frequencies of 1 to 30 Hz. The green arrow indicates the a-wave, and the purple arrow indicates the b-wave.

## Stimulation and Recording

We used standard light-[45] and dark-adapted[46] protocols based on ISCEV standards. For the light-adapted protocol, 4-ms green flashes of 9 incrementing steps ranging from 0.16 to 30 cd·s/m$^2$ were presented on a green rod-suppressing background of 30 cd/m$^2$ and adapted for 10 minutes prior to recording. Twenty-five responses were collected per step, with a 5- to 10-second interstep and 10-second interstimulus interval. For the mesopic-adapted protocol, 4-ms white flashes of 7 incrementing steps ranging from 0.175 to 11.2 cd·s/m$^2$ were presented on a white background luminance of 0.1 cd/m$^2$ and adapted for 10 minutes prior to recording. Four responses were collected per step, with a 10-second interstep and 10-second interstimulus intervals. For the dark-adapted protocol, 4-ms blue flashes of 7 incrementing steps ranging from 0.00025 to 1 cd·s/m$^2$ without background luminance were used, and mice were dark-adapted overnight prior to the experiments. Sixteen responses were collected per step, with a 10-second interstep and 10-second interstimulus interval. Collected responses were averaged to attain representative traces at each light intensity for each animal. Data were collected using the Espion E$^2$ Console Model D215 (Diagnosys LLC, Lowell, MA, USA) with a 0.3-Hz bandpass filter. Mice were anesthetized with 4% isoflurane gas, and anesthesia was maintained with 1.7% isoflurane. Isoflurane was selected as the anesthetic of choice because the combination of ketamine and xylazine blocks NMDAR receptor transmission, as ketamine is an NMDAR non-competitive antagonist.[58] Because we measured the functionality in mice with NMDAR hypofunction, ketamine as an anesthetic would have confounded the results. Previous literature supported isoflurane as an effective anesthetic agent for maintaining normal mouse fERGs.[59] After anesthetic, tropicamide (1%) eye drops (Akorn Inc., Lake Forest, IL, USA) were used as a pupil dilator, followed by corneal analgesic proparacaine hydrochloride eye drops (0.5%) (Akorn). A heating pad was used to maintain the mouse body temperature at 37°C. A contact lens coiled wire electrode was placed on the cornea and embedded in methylcellulose (1.0%) eye drops (Allergan, Dublin, Ireland).[59]

## Fourier Transform Analysis

A custom MATLAB program was used to determine the spectral content on fERGs via fast Fourier transform (FFT). Four traces collected at each light intensity were converted into power spectra using FFT and then averaged together for every animal. From these averaged power spectra, low-frequency content was taken by averaging the spectra from 0 to 30 Hz.

Investigative Ophthalmology & Visual Science

### Data Analysis

To remove OP contamination from the a- and b-wave measurements, each ERG response was filtered using a low-pass filter with a passband of 50 Hz and stopband of 65Hz using a custom MATLAB program.[60,61] The four filtered traces corresponding to a given light intensity for each animal were averaged and smoothed in MATLAB. Using this filtered ERG, the a-wave amplitude was measured from the pre-flash baseline to the peak of the a-wave, and the b-wave amplitude was measured from the peak of the a-wave (trough) to the largest peak of the b-wave. Implicit time of the a-wave and b-wave was measured from flash onset to response peak. Normality was tested using the Shapiro–Wilk's test ($P > 0.05$) for each group at each level of light intensity in each of the light-adapting conditions. In the mesopic dataset, female $SR^{-/-}$ a-wave amplitudes were not normally distributed at the dimmest light intensities, 0.175 and 0.35. Female WT a-wave amplitudes were not normally distributed at a light intensity of 0.35. The b-wave amplitudes were not normally distributed at the dimmest light intensity (0.175) of female $SR^{-/-}$. In the dark-adapted dataset there was one outlier, a female $SR^{-/-}$, that was removed from the analysis as data points were 3 standard deviations away from the mean. Including or excluding this animal from analysis did not change the statistical analysis of the dark-adapted fERGs.

Aside from the aforementioned data points, the remaining light intensities across groups were normally distributed. Two-factor between-subject analysis of variance (ANOVA) was conducted to evaluate a potential significant interaction between the independent variables sex and genotype and the simple main effects of sex (male [m] vs. female [f]) and genotype (WT vs. $SR^{-/-}$) in the mesopic dataset. One-way ANOVA was performed for the fWT, f$SR^{-/-}$, mWT, and m$SR^{-/-}$ groups for light- and dark-adapted datasets. Finally, we carried out a two-way mix ANOVA (light intensity*sex) and (light intensity*genotype) to account for changes in light intensity, the repeated measure for all mice, in all dependent variables. The dependent variables tested were a-wave amplitude and implicit time, b-wave amplitude and implicit time, b-/a-wave ratio, and Fourier transforms. All analyses were conducted for each light intensity. If there was a statistically significant two-way ANOVA difference, analysis for the simple main effects of the given dependent variable was performed using a Bonferroni adjustment with statistical significance at $P < 0.025$. To evaluate the effect of genotype or sex alone, the main effects were analyzed through differences between the unweighted marginal means. All analyses were conducted using SPSS Statistics 26 (IBM, Armonk, NY, USA).

### Retinal Histology and Immunocytochemistry

To assess if there were significant changes in overall morphology of the retina from the $SR^{-/-}$ mice compared to WT, three eyes from three animals per genotype were removed after euthanasia, fixed in 4% phosphate-buffered paraformaldehyde (Affymetrix, Cleveland, OH, USA), and post-fixed in paraformaldehyde for several hours, followed by rinses in PBS and incubation overnight in 10% sucrose in PBS and 20% sucrose in PBS. The eyes were embedded in paraffin and sectioned at 10 µm on a sliding microtome. The sections were stained with hematoxylin and eosin by standard procedures. Sections through the optic nerve head and through a defined location in peripheral retina, based on the anterior appearance of the ciliary body and cornea in the sections (see Supplemental Fig. S3), were used for measurements in order to be consistent where our measurements were taken. A BIOQUANT Image Analysis System (BIOQUANT Image Analysis Corporation, Nashville, TN, USA) was used to determine the mean height of each of the layers of the retina with three separate measurements per layer per area in the central retina and a mean of six measurements of the retinal layers in peripheral retina in two locations. These data were analyzed using unpaired *t*-tests for each layer and each region, with significance at $P < 0.05$.

A second series of retinas were removed and frozen in 2-methylbutane in liquid nitrogen and sectioned at 12 µm in a cryostat. Sections were prepared from three eyes from three mice per genotype. The sections were immunostained with antibodies specific for D-serine (1:200, #ab6472, Abcam, Cambridge, UK) or serine racemase (1:200, #ab224620, Abcam) and the VectaFluor Excel Amplified DyLight 488 Anti-Rabbit IgG Kit (Vector Laboratories Inc., Burlingame, CA, USA). The slides were then immunostained for either brn3a, a ganglion cell-specific marker (1:50, #sc-8429, Santa Cruz Biotechnology, Dallas, TX, USA) or CHX10 (1:100, #ab16141, Abcam), a bipolar-cell-specific marker. For brn3a, this was followed by incubation with a goat anti-mouse IgG secondary antibody conjugated to Cy3 (1:500, Jackson Immunoresearch Laboratories, West Grove, PA, USA); for CHX10, the slides were incubated in a donkey anti-sheep IgG secondary antibody conjugated to Cy3 (1:500, Jackson Immunoresearch). Sections were coverslipped and examined with fluorescence microscopy.

Using the thresholding program in BIOQUANT, the overall intensities of green labeling in three sections per eye were determined, and the average of these were used to generate a mean fluorescence intensity. Means for each of the three eyes per genotype per primary antibody were determined, and statistical differences were determined using a Student's *t*-test. Values are given as percent of positive area per total area of the given microscopic field. Co-labeling of ganglion cells with D-serine and serine racemase was determined using fluorescence microscopy.

## Results

### Effect of NMDAR Hypofunction on the a-Wave Amplitude

Representative fERG traces from mesopic (Fig. 1) and light- and dark-adapted (Supplementary Fig. S1) male and female WT and $SR^{-/-}$ are displayed as waveforms at each light intensity. Analysis of the mesopic a-wave amplitude showed no statistically significant difference between WT and $SR^{-/-}$ mice (Supplementary Fig. S2A, Supplementary Table S1). Analysis of genotype for male mice showed that the a-wave amplitudes were significantly different only at the highest intensity (Supplementary Fig. S2B), whereas female mice showed a significant difference at the lowest light intensity (Supplementary Fig. S2C). Significance at the brightest intensity was similar to the ERG in a study of individuals with schizophrenia.[2] Analysis of dark- and light-adapted a-wave amplitudes between groups showed no significant differences (Supplementary Figs. S2D, S2E; Supplementary Table S2).

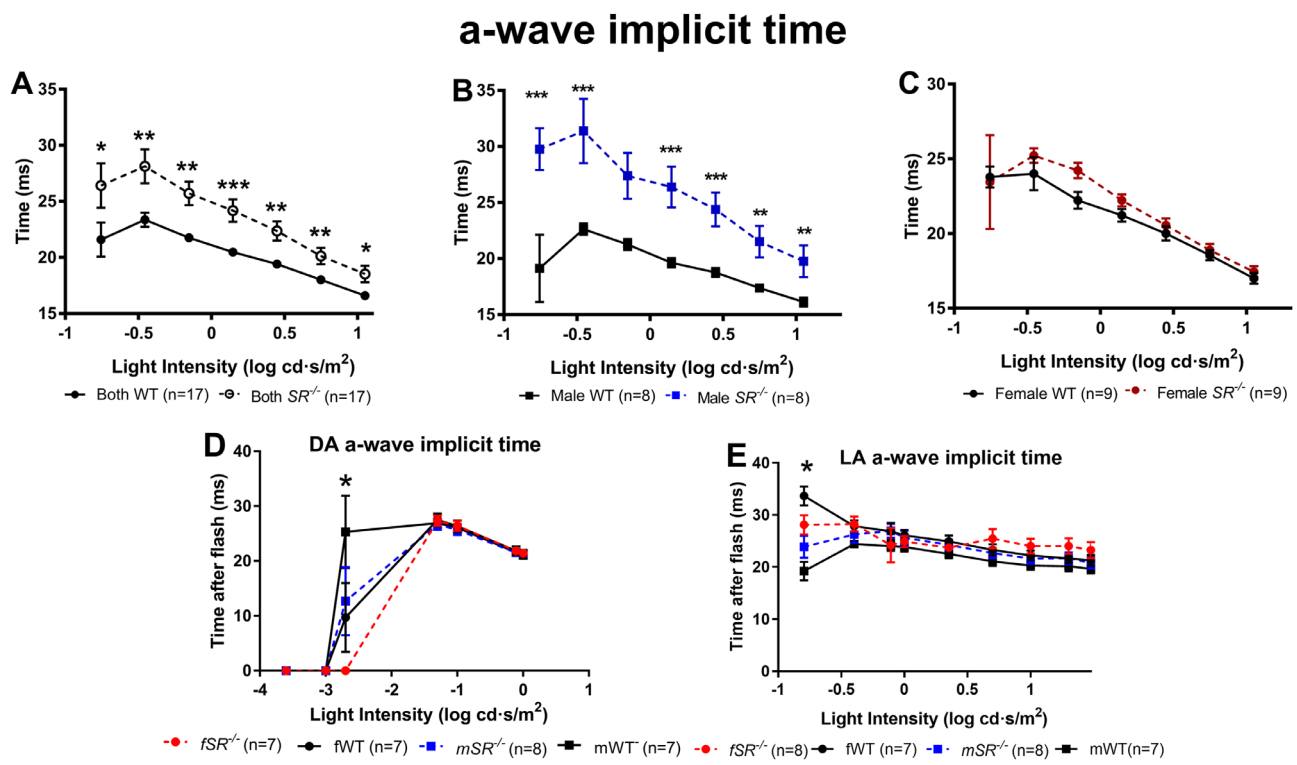


**Figure 2.** a-Wave implicit time analysis. (A) Mesopic adaptation: comparison of a-wave implicit time based on genotype and evaluation of the main effects; WT (black), $SR^{-/-}$ (gray). (B, C) Comparison of genotype for a specific gender evaluating the simple main effects of sex. Male mice (B; blue line) and female mice (C; red line) at all light intensities; WT (black) and $SR^{-/-}$ mice. (D) Dark-adapted (DA) a-wave implicit time and (E) light-adapted (LA) a-wave implicit time for the four groups: female WT (black line circles), female $SR^{-/-}$ (red line circles), male WT (black line squares), and male $SR^{-/-}$ (blue line squares). Data are expressed as mean (line), SEM (error bars), and significance ($^{*}P$ = 0.05–0.01; $^{**}P$ = 0.001–0.005; $^{***}P < 0.0005$). * indicates the results are significant, but missing data points due to lack of detectable a-waves in 1 or 2 animals at that light intensity.

**Table 1.** Comparison of a-Wave Implicit Times in WT and $SR^{-/-}$ Mice

| Flash Intensity (cd·s/m²) | a-Wave Implicit Time (ms) | | Main Effects Genotype |
|---|---|---|---|
| | WT | $SR^{-/-}$ | |
| 0.175 | 22 ± 6.3 | 26 ± 8.2 | $F(1, 30) = 4.7$, $P = 0.039$ |
| 0.35 | 23 ± 2.6 | 28 ± 6.3 | $F(1, 30) = 11.0$, $P = 0.002$ |
| 0.7 | 22 ± 1.6 | 26 ± 4.3 | $F(1, 30) = 14.3$, $P = 0.001$ |
| 1.4 | 20 ± 1.5 | 24 ± 4.1 | $F(1, 30) = 17.4$, $P < 0.0005$ |
| 2.8 | 19 ± 1.4 | 22 ± 3.6 | $F(1, 30) = 14.7$, $P = 0.001$ |
| 5.6 | 18 ± 1.2 | 20 ± 3.1 | $F(1, 30) = 9.1$, $P = 0.005$ |
| 11.2 | 17 ± 1.2 | 19 ± 3.0 | $F(1, 30) = 7.4$, $P = 0.011$ |

Data represent a-wave implicit times given genotype, with data from males and females pooled. Data are expressed as mean ± SD. The *P* values are the results of main effects analysis.

## Significant Effect of NMDAR Hypofunction on the Mesopic a-Wave Implicit Time

The a-wave implicit time of the mesopic fERGs was significantly delayed in $SR^{-/-}$ mice compared to WT mice at all light intensities, with the $SR^{-/-}$ mice significantly delayed compared to the normal WT a-wave (Fig. 2A, Table 1). The simple main effect for sex revealed that $SR^{-/-}$ male mice had a significantly delayed a-wave implicit time in comparison to male WT at all light intensities except one (Fig. 2B, Table 2), whereas there were no significant differences in the a-wave implicit time between female WT and $SR^{-/-}$ mice (Fig. 2C). However, a-wave implicit time of light- and dark-adapted fERGs was not significant between groups (Figs. 2D, 2E).

## Significant Effect of NMDAR Hypofunction on the Mesopic b-Wave Amplitude

The b-wave amplitude in $SR^{-/-}$ mice was profoundly reduced in the mesopic-adapted fERGs (Fig. 3A), whereas it remained mostly unchanged in light- and dark-adapted fERGs (Figs. 3D, 3E). On the other hand, the mesopic b-wave amplitude differed significantly between WT and $SR^{-/-}$ mice (Fig. 3). Analysis of the main effects showed that the b-wave amplitudes were significantly reduced at every light intensity between the $SR^{-/-}$ and WT mice. $SR^{-/-}$ mice had a reduced b-wave amplitude ranging from 21 to 62 µV depending on light intensity and, interestingly, did not change when light intensity was increased (Fig. 3A, Table 3). Examination of the simple main effects was conducted to evaluate whether members of the same sex but opposing genotypes were different from one another. The simple main effect for sex revealed that $SR^{-/-}$ male mice had significantly smaller b-wave amplitudes in comparison to male WT mice at all light intensities except the highest (Fig. 3B, Table 4). Female mice showed a decrease in b-wave amplitude for 4 of the 7 light intensities (Fig. 3C). Simple main effects of genotype were determined to understand whether mice of the same genotype, but opposite sex, differed from one another. Male mice had statistically higher b-wave amplitudes in comparison to females (Table 4), whereas the $SR^{-/-}$ female

Investigative Ophthalmology & Visual Science

**Table 2.** Comparison of a-Wave Implicit Time in WT and $SR^{-/-}$ Mice Depending on Sex

| Flash Intensity ($cd{\cdot}s/m^2$) | a-Wave Time (ms) | | | | | | |
|---|---|---|---|---|---|---|---|
| | Female | | Male | | | Simple Main Effects | |
| | WT | $SR^{-/-}$ | WT | $SR^{-/-}$ | Interaction Sex*Genotype | Sex | Genotype |
| 0.175 | 24 | 23 | 19 | 30 | $F(1, 30) = 5.3$, $P = 0.029$ | Male: $P < 0.0005$ | NS |
| 0.35 | 24 | 25 | 23 | 31 | $F(1, 30) = 6.2$, $P = 0.018$ | Male: $P < 0.0005$ | $SR^{-/-}$: $P = 0.007$ |
| 0.7 | 22 | 24 | 21 | 27 | $F(1, 30) = 3.7$, $P = 0.064$ | NA | NA |
| 1.4 | 21 | 22 | 20 | 26 | $F(1, 30) = 9.6$, $P = 0.004$ | Male: $P < 0.0005$ | $SR^{-/-}$: $P = 0.004$ |
| 2.8 | 20 | 21 | 19 | 24 | $F(1, 30) = 9.9$, $P = 0.004$ | Male: $P < 0.0005$ | $SR^{-/-}$: $P = 0.002$ |
| 5.6 | 19 | 19 | 17 | 22 | $F(1, 30) = 6.6$, $P = 0.016$ | Male: $P < 0.001$ | $SR^{-/-}$: $P = 0.018$ |
| 11.2 | 17 | 17 | 16 | 20 | $F(1, 30) = 4.5$, $P = 0.042$ | Male: $P < 0.002$ | $SR^{-/-}$: $P = 0.038$ |

The first two columns represent the mean a-wave implicit time at each condition. The interaction column includes the results from the analysis examining the interaction between sex and genotype with its corresponding *P* values. The simple main effects for sex and genotype are shown in the last two columns with *P* values Bonferroni-adjusted within each simple main effect. NA, not applicable; NS, not significant.

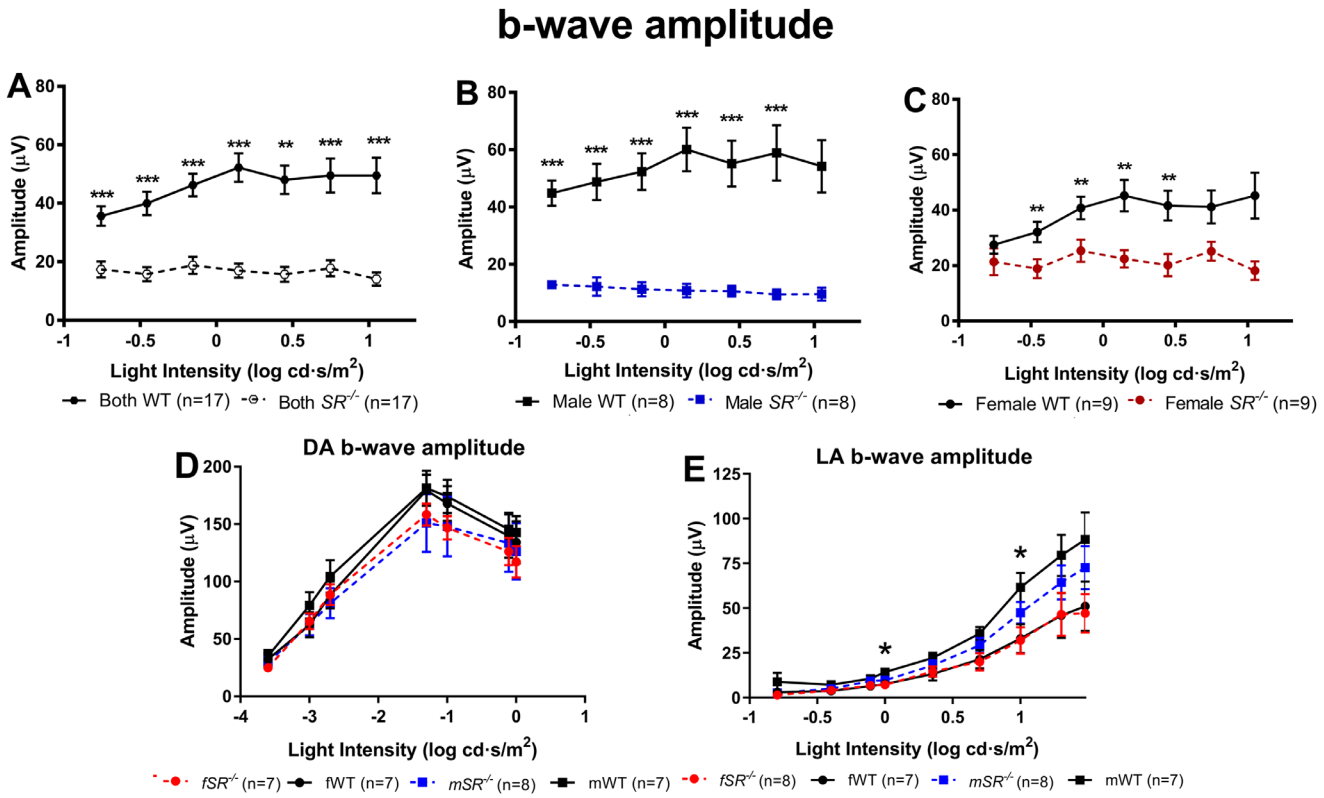


**Figure 3.** b-Wave amplitude analysis. (A) Mesopic adaptation: comparison of b-wave amplitude based on genotype and evaluation of the main effects; WT (black), $SR^{-/-}$ (gray). (B, C) Mesopic adaptation: comparison of genotype for a specific gender evaluating the simple main effects of sex. Male mice (B; blue line) and female mice (C; red line) at all light intensities; WT (black) and $SR^{-/-}$ mice. (D) Dark-adapted (DA) b-wave amplitude and (E) light-adapted (LA) b-wave amplitude for the four groups: female WT (black line circles), female $SR^{-/-}$ (red line circles), male WT (black line squares), and male $SR^{-/-}$ (blue line squares). Data are expressed as mean (line), SEM (error bars), and significance ($^{*}P = 0.05$–$0.01$; $^{**}P = 0.001$–$0.005$; $^{***}P < 0.0005$).

and $SR^{-/-}$ male mice were not statistically different from one another. A two-way mixed ANOVA was performed to understand if there was an interaction between sex with repeated changes in light intensity and between genotype and repeated changes in light intensity. No dependent variables were significant for sex and light intensity interaction; however, b-wave amplitude was the only dependent variable that showed significant differences between light intensity and genotype ($df[6, 180] = 4.6$; $P < 0.0005$). These results suggest that the $SR^{-/-}$ mice b-wave amplitude did not modulate to increasing light intensity. The dark-adapted b-wave amplitude was not significant across groups, and the light-adapted b-wave amplitude was only significant at two light intensities (Fig. 3E, Supplementary Table S3).

These results demonstrate that at all light intensities, the D-serine deficiency resulting in NMDAR hypofunction reduced the b-wave amplitude under mesopic conditions. However, this reduction in amplitude depended on whether the animal was male or female. Male $SR^{-/-}$ mice exhibited a statistically significant reduction in b-wave amplitude in comparison to WT males across light intensities; however, only at the middle light intensities were the $SR^{-/-}$ females

Investigative Ophthalmology & Visual Science

**Table 3.** Comparison of b-Wave Amplitude in WT and $SR^{-/-}$ Mice

| Flash intensity (cd·s/m$^2$) | b-Wave Amplitude (μV) | | Main Effects Genotype |
|---|---|---|---|
| | WT | $SR^{-/-}$ | |
| 0.175 | 36 ± 14.0 | 17 ± 11.3 | $F(1, 30) = 25.7$, $P < 0.0005$ |
| 0.35 | 40 ± 16.7 | 16 ± 9.9 | $F(1, 30) = 33.6$, $P < 0.0005$ |
| 0.7 | 46 ± 16.0 | 19 ± 12.1 | $F(1, 30) = 40.3$, $P < 0.0005$ |
| 1.4 | 52 ± 20.2 | 17 ±10.0 | $F(1, 30) = 49.8$, $P < 0.0005$ |
| 2.8 | 48 ± 20.1 | 16 ± 10.4 | $F(1, 30) = 39.4$, $P < 0.0005$ |
| 5.6 | 50 ± 23.9 | 18 ± 11.3 | $F(1, 30) = 30.9$, $P < 0.0005$ |
| 11.2 | 49 ± 25.0 | 14 ± 9.4 | $F(1, 30) = 30.4$, $P < 0.0005$ |

Data represent b-wave amplitude for each genotype; male and female data are pooled. Data are expressed as mean ± SD. The *P* values are the results of main effects analysis.

statistically lower than the WT females. Interestingly, the b-wave amplitudes between $SR^{-/-}$ male and $SR^{-/-}$ female mesopic b-wave amplitudes were not statistically significantly different from one another; however, in WT female and WT male mice they differed at lower light intensities. This highlights the importance of investigating gender differences in fERGs of WT animals as well as genetically modified mice.

## Significant Effect of NMDAR Hypofunction on the Mesopic b-Wave Implicit Time

The b-wave implicit time was largely delayed in the $SR^{-/-}$ mice in the mesopic condition but remained the same across groups in the dark- and light-adapted conditions. The mesopic b-wave implicit times for the $SR^{-/-}$ mice were significantly delayed from those generated by WT retinas at all light intensities (Fig. 4A, Table 5). There was an interaction effect between sex and genotype at the brightest light intensities (Table 6). $SR^{-/-}$ males had a statistically significant delay in the b-wave implicit time in the brightest light intensities in comparison to WT male mice (Fig. 4B, Table 6). This difference was not present in the female mice (Fig. 4C). Comparing the b-wave implicit time for members of the same genotype but opposing sex, $SR^{-/-}$ male and female mice differed at the brightest light intensities, with male mice having a statistically greater delay in the b-wave implicit time (Table 6), whereas WT female and WT male mice did not differ from one another. This demonstrates that the peak of the b-wave in $SR^{-/-}$ mice occurs later in time after flash onset compared to WT mice. However, this delay in the b-wave implicit time depended on the light intensity and sex of the animal. At brighter light intensities, $SR^{-/-}$ male mice had a statistically significant delay in the b-wave implicit time in comparison to all other groups (Table 6). There were no significant differences in b-wave implicit time across groups in the dark- and light-adapted conditions (Figs. 4D, 4E).

## Significant Effect of NMDAR Hypofunction on the Mesopic b-/a-Wave Ratio

Because the amplitude of the mesopic b-wave depended on the interaction between sex and genotype at all light intensities and the a-wave amplitude did not (Supplementary Fig. S2, Supplementary Table S1), we calculated the b-/a-wave ratio to determine whether the relationship between the a- and b-wave differences depended on the interaction of genotype and sex. At all light intensities except the lowest, the b-/a-wave ratio was significantly reduced in $SR^{-/-}$ mice in comparison to WT mice (Fig. 5, Table 7). There was no interaction effect between sex and genotype (analysis not shown). In sum, the b-/a-wave ratio quantification in the mesopic fERGs demonstrated a reduction in the $SR^{-/-}$ mice, regardless of the sex of the animal. This is the first use of the b-/a-ratio in analysis of the ERG from an animal model or from humans with schizophrenia. It will be important to see if these differences are seen in people with schizophrenia. There were almost no significant differences in the b-/a-wave ratio in the dark- and light-adapted conditions (Figs. 5D, 5E).

## Fourier Transform Analysis for the Mesopic ERGs

Fourier transform analysis decomposes a signal into contributing frequency components and provides the weight (power) that each frequency contributes to the original signal. Fourier transform analysis on the low-frequency components of the fERG, the a- and b-waves, showed a statistically significant reduction in $SR^{-/-}$ mice in comparison to WT mice at all light intensities except the dimmest light values (Fig. 6A, Table 8). There was a significant interaction between genotype and sex at the three lowest light intensities (valuemin – valuemax) (Table 9). Examination of

**Table 4.** Comparison of b-Wave Amplitude in WT and $SR^{-/-}$ Mice Depending on Sex

| Flash Intensity (cd·s/m$^2$) | b-Wave Amplitude (μV) | | | | Interaction Sex*Genotype | Simple Main Effects | |
|---|---|---|---|---|---|---|---|
| | Female | | Male | | | Sex | Genotype |
| | WT | $SR^{-/-}$ | WT | $SR^{-/-}$ | | | |
| 0.175 | 27 | 21 | 45 | 13 | $F(1, 30) = 11.8$, $P = 0.002$ | Male: $P < 0.0005$, Female: $P$ = NS | WT: $P = 0.003$ |
| 0.35 | 32 | 19 | 49 | 12 | $F(1, 30) = 7.4$, $P = 0.011$ | Male: $P < 0.0005$, Female: $P = 0.032$ | WT: $P = 0.010$ |
| 0.7 | 41 | 25 | 52 | 11 | $F(1, 30) = 8.3$, $P = 0.007$ | Male: $P < 0.0005$, Female: $P = 0.017$ | WT: $P = 0.075$ |
| 1.4 | 45 | 22 | 60 | 11 | $F(1, 30) = 6.7$, $P = 0.015$ | Male: $P < 0.0005$, Female: $P = 0.003$ | WT: $P = 0.048$ |
| 2.8 | 41 | 20 | 55 | 11 | $F(1, 30) = 4.8$, $P = 0.036$ | Male: $P < 0.0005$, Female: $P = 0.006$ | WT: $P = 0.080$ |
| 5.6 | 41 | 25 | 59 | 9 | $F(1, 30) = 8.1$, $P = 0.008$ | Male: $P < 0.0005$, Female: $P$ = NS | WT: $P = 0.041$ |
| 11.2 | 45 | 18 | 54 | 10 | $F(1, 30) = 1.8$, $P = 0.188$ | NA | NA |

Columns 2 to 5 represent the mean b-wave amplitude for each condition. The interaction column includes the results from the interaction between sex and genotype with the corresponding *P* values. The simple main effects analysis for sex and genotype are shown in the last two columns with *P* values Bonferroni-adjusted within each simple main effect. NA, not applicable; NS, not significant.

Investigative Ophthalmology & Visual Science

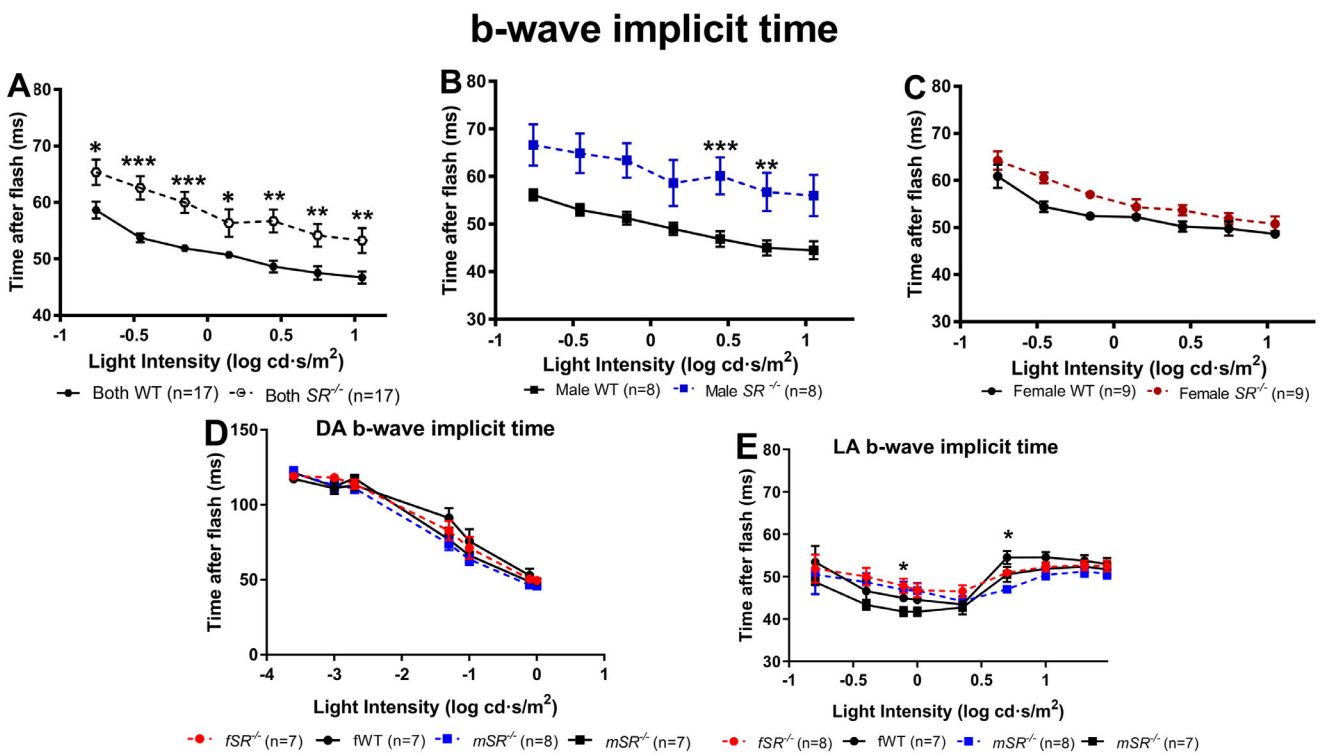


**Figure 4.** b-Wave implicit time analysis. (A) Mesopic adaptation: comparison of b-wave implicit time based on genotype and evaluation of the main effects; WT (black), $SR^{-/-}$ (gray). (B, C) Mesopic adaptation: comparison of genotype for a specific gender evaluating the simple main effects of sex. Male mice (B; blue line) and female mice (C; red line) at all light intensities; WT (black) and $SR^{-/-}$ mice. (D) Dark-adapted b-wave implicit time and (E) light-adapted b-wave implicit time for the four groups: female WT (black line circles), female $SR^{-/-}$ (red line circles), male WT (black line squares), male $SR^{-/-}$ (blue line squares). Data are expressed as mean (line), SEM (error bars), and significance ($^{*}P = 0.05$–$0.01$; $^{**}P = 0.001$–$0.005$; $^{***}P < 0.0005$).

the simple main effects was conducted to evaluate whether members of the same sex but opposing genotypes were different from one another. The simple main effect for sex revealed that $SR^{-/-}$ male mice had a significantly smaller low-frequency component in comparison to male WT at all light intensities (Figs. 6B, 6C; Table 9). There was no statistically significant difference between $SR^{-/-}$ and WT females (Figs. 5D, 5E). Analysis of the low-frequency component demonstrated that $SR^{-/-}$ mice had lower power in comparison to WT mice, but this difference was greater in males at the lowest light intensities.

**Table 5.** Comparison of b-Wave Implicit Time in WT and $SR^{-/-}$ Mice

| Flash intensity (cd·s/m²) | b-Wave Implicit Time (ms) | | Main Effects Genotype |
|---|---|---|---|
| | WT | $SR^{-/-}$ | |
| 0.175 | 59 ± 6.2 | 65 ± 9.2 | $F(1, 30) = 6.6$, $P = 0.016$ |
| 0.35 | 54 ± 3.4 | 63 ± 8.5 | $F(1, 30) = 16.3$, $P < 0.0005$ |
| 0.7 | 52 ± 3.2 | 60 ±7.8 | $F(1, 30) = 18.6$, $P < 0.0005$ |
| 1.4 | 51 ± 3.2 | 56 ± 10 | $F(1, 30) = 5.3$, $P = 0.028$ |
| 2.8 | 49 ± 4.2 | 57 ± 8.4 | $F(1, 30) = 15.0$, $P = 0.001$ |
| 5.6 | 48 ± 5.1 | 54 ± 8.3 | $F(1, 30) = 9.3$, $P = 0.005$ |
| 11.2 | 47 ± 4.4 | 53 ± 9.2 | $F(1, 30) = 8.0$, $P = 0.008$ |

Data represent the b-wave implicit time for each genotype; male and female data are pooled. Data are expressed as mean of each genotype ± SD. The *P* values are the results of main effects analysis.

## Morphometric Analysis of Retinal Layer Thickness in $SR^{-/-}$ and WT mice

The thickness of each layer of the retina in both the central and peripheral retina from $SR^{-/-}$ and WT mice were analyzed for differences due to loss of D-serine in the $SR^{-/-}$ mice. No significant differences were seen in any of the layers of either the central or peripheral retina (Supplementary Fig. S3). It should be noted that these mice were generated and validated in the Coyle laboratory, where they were shown to mimic a number of aspects of the human disease.[10] The retinas of these mice were shown to have significantly reduced D-serine concentration, as measured by capillary electrophoresis, and both significantly reduced co-agonist occupancy of the NMDAR and a significant reduction in the NMDAR component of ganglion cell light-evoked responses with retention of normal vision as measured by the optokinetic reflex.[62]

## Immunocytochemical Analysis of D-Serine and Serine Racemase Expression in the $SR^{-/-}$ and WT Mice

Quantification of the levels of D-serine and serine racemase were determined using the densitometry function in our morphometry system. In the $SR^{-/-}$ mice, D-serine levels were significantly lower, and serine racemase was not detectable by our densitometric system (Figs. 7A, 7B).

Immunohistochemical examination showed a confirmatory reduction in the levels of D-serine in the $SR^{-/-}$ mice

**Table 6.** Comparison of b-Wave Implicit Time in WT and $SR^{-/-}$ Mice Depending on Sex

| Flash Intensity ($cd \cdot s/m^2$) | b-Wave Implicit Time (ms) | | | | | | |
|---|---|---|---|---|---|---|---|
| | Female | | Male | | | Simple Main Effects | |
| | WT | $SR^{-/-}$ | WT | $SR^{-/-}$ | Interaction Sex*Genotype | Sex | Genotype |
| 0.175 | 61 | 64 | 56 | 67 | $F(1, 30) = 1.8$, $P$ = NS | NA | NA |
| 0.35 | 54 | 61 | 53 | 65 | $F(1, 30) = 1.7$, $P$ = NS | NA | NA |
| 0.7 | 52 | 57 | 51 | 63 | $F(1, 30) = 3.8$, $P$ = NS | NA | NA |
| 1.4 | 52 | 54 | 49 | 59 | $F(1, 30) = 2.2$, $P$ = NS | NA | NA |
| 2.8 | 50 | 54 | 47 | 60 | $F(1, 30) = 5.2$, $P = 0.030$ | Male: $P < 0.0005$ | $SR^{-/-}$: $P = 0.043$ |
| 5.6 | 50 | 52 | 45 | 57 | $F(1, 30) = 4.5$, $P = 0.043$ | Male: $P = 0.001$ | NS |
| 11.2 | 49 | 51 | 45 | 56 | $F(1, 30) = 3.8$, $P$ = NS | NA | NA |

The first two columns represent the mean b-wave implicit time each condition. The interaction column includes the results from the interaction between sex and genotype with its corresponding $p$-values. Simple main effects analysis for sex (SME: Sex) and genotype (SME: Genotype) are in the last two columns with $p$-values Bonferroni-adjusted within each simple main effect. (N.A.) stands for not applicable.

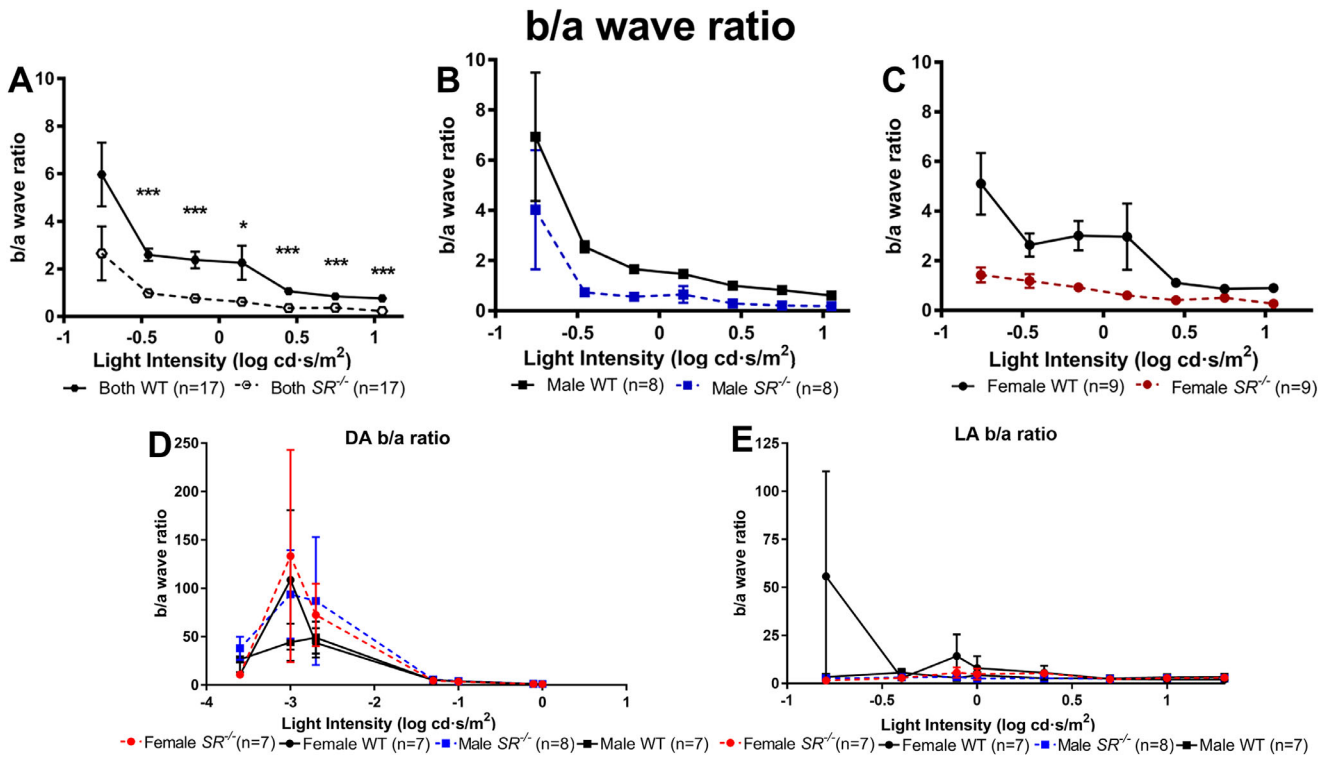


**Figure 5.** b-/a-Wave ratio analysis. (A) Mesopic adaptation: comparison of b-/a-wave ratio based on genotype and evaluation of the main effects; WT (black), $SR^{-/-}$ (gray). (B, C) Mesopic adaptation: comparison of genotype for a specific gender evaluating the simple main effects of sex. Male mice (B; blue line) and female mice (C; red line) at all light intensities; WT (black) and $SR^{-/-}$ mice. (D) Dark-adapted b-/a-wave ratio and (E) light-adapted b-/a-wave ratio for the four groups: female WT (black line circles), female $SR^{-/-}$ (red line circles), male WT (black line squares), and male $SR^{-/-}$ (blue line squares). Data are expressed as mean (line), SEM (error bars), and significance ($^{*}P = 0.05$–$0.01$; $^{**}P = 0.001$–$0.005$; $^{***}P < 0.0005$).

compared to WT mice (Figs. 7B–7D). Both bipolar cells (Figs. 7C, 7D) and ganglion cells (Figs. 7E, 7F) were positive for D-serine expression (Figs. 7B, 7C) and serine racemase expression (not shown).

## Discussion

This study demonstrated that fERGs in a mouse model of schizophrenia with hypofunction of the NMDAR had a smaller b-wave amplitude, delayed a-wave and b-wave implicit time, smaller b-/a-wave ratio, and a decreased low-frequency component of the Fourier transform analysis only in mesopic-adapted fERGs, whereas light- and dark-adapted fERGs remained largely unaffected. This highlights the potential of using mesopic background luminance specifically in the identification of abnormalities pertinent to schizophrenic pathology. Similar to people with schizophrenia, mice with NMDAR hypofunction had a reduced b-wave amplitude and delayed b-wave implicit time in comparison to controls. However, we emphasize that this reduction depended on light adaptation and whether the mouse was

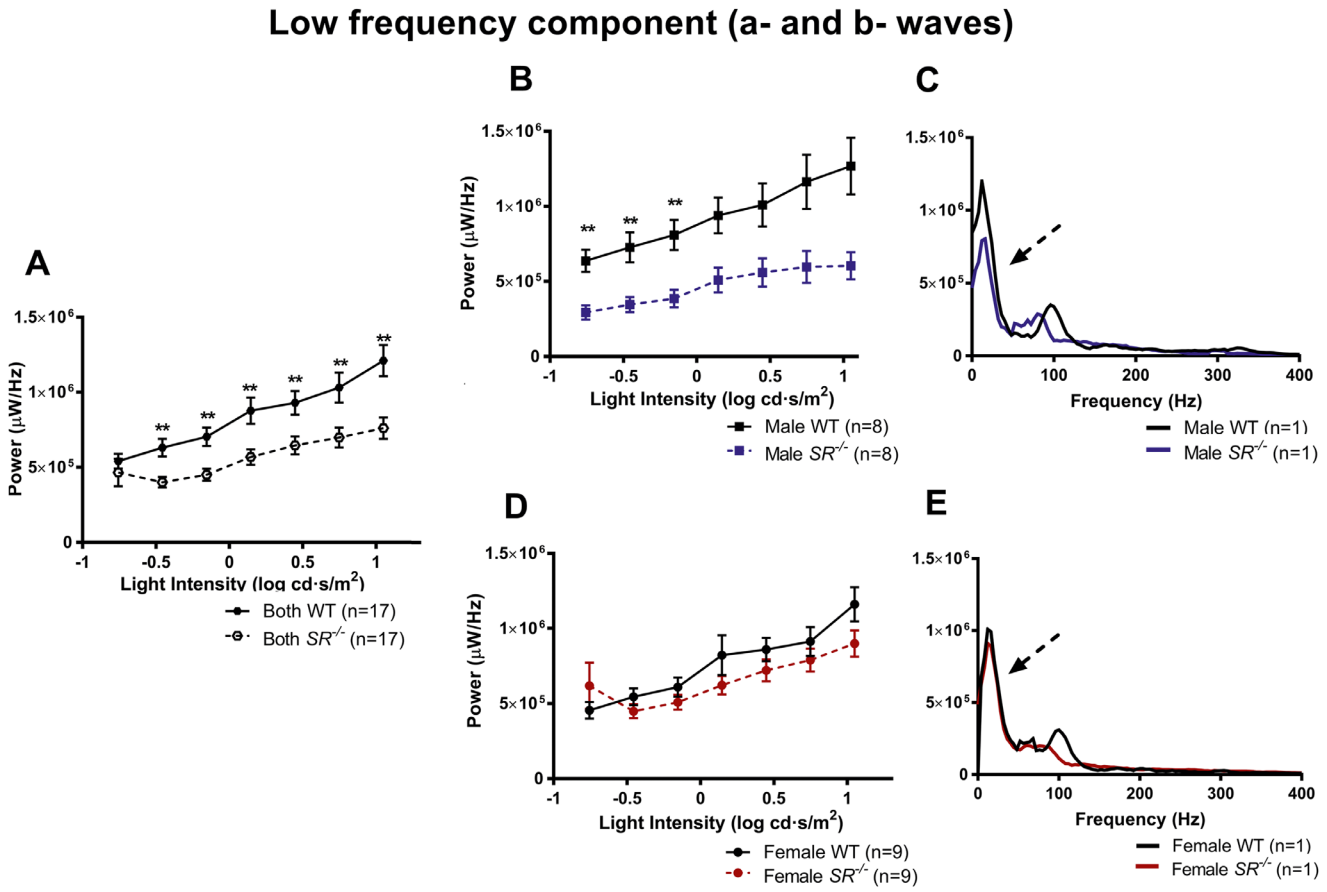


**Figure 6.** Fast Fourier transform analysis in males and females of WT (black) and $SR^{-/-}$ mice (males, blue line; females, red line) of the mesopic a- and b-waves at all light intensities. Sample Fourier transform output of one animal per given genotype at light intensity 5.62 cd·s/m$^2$ is shown for males (C) and females (E). The black dashed arrow points to the low-frequency component. (A) Comparison of the low-frequency component given genotype by evaluating the main effects (WT, solid line and closed circles; $SR^{-/-}$, dashed line and open circles). $SR^{-/-}$ mice had a reduced low-frequency component in comparison to WT at the dimmest light intensities in the males (B) but not females (D). Data are expressed as mean (line), SEM (error bars), and significance ($^{*}P$ = 0.05–0.01; $^{**}P$ = 0.001–0.005; $^{***}P < 0.0005$).

**Table 7.** Comparison of the b/a Wave Ratio in WT and $SR^{-/-}$ Mice Depending on Sex

| Flash Intensity (cd·s/m$^2$) | b-/a-Wave Ratio | | Main Effects Genotype |
|---|---|---|---|
| | WT | $SR^{-/-}$ | |
| 0.175 | 6 ± 5.6 | 3 ± 4.7 | $F(1, 30) = 3.4$, $P = 0.074$ |
| 0.35 | 3 ± 1.1 | 1 ± 0.7 | $F(1, 30) = 26.5$, $P < 0.0005$ |
| 0.7 | 2 ± 1.5 | 0.8 ± 0.5 | $F(1, 30) = 22.3$, $P < 0.0005$ |
| 1.4 | 2 ± 2.9 | 0.6 ± 0.7 | $F(1, 30) = 4.7$, $P = 0.038$ |
| 2.8 | 1 ± 0.4 | 0.4 ± 0.2 | $F(1, 30) = 38.2$, $P < 0.0005$ |
| 5.6 | 0.8 ± 0.2 | 0.4 ± 0.2 | $F(1, 30) = 37.8$, $P < 0.0005$ |
| 11.2 | 0.8 ± 0.4 | 0.2 ± 0.1 | $F(1, 30) = 25.6$, $P < 0.0005$ |

Data represent the b/a wave ration for each genotype. Data are expressed as the mean of each genotype. The *P* values are the results of main effects analysis.

**Table 8.** Comparison of Low Frequency Component in WT and $SR^{-/-}$ Mice

| Flash Intensity (cd·s/m$^2$) | WT | $SR^{-/-}$ | Main Effects Genotype |
|---|---|---|---|
| 0.175 | $5.4 \times 10^5$ | $4.7 \times 10^5$ | $F(1, 30) = 0.874$, $P = 0.357$ |
| 0.35 | $4.0 \times 10^5$ | $6.3 \times 10^5$ | $F(1, 30) = 13.3$, $P = 0.001$ |
| 0.7 | $7.0 \times 10^5$ | $4.5 \times 10^5$ | $F(1, 30) = 14.1$, $P = 0.001$ |
| 1.4 | $8.8 \times 10^5$ | $5.7 \times 10^5$ | $F(1, 30) = 9.3$, $P = 0.005$ |
| 2.8 | $9.3 \times 10^5$ | $6.5 \times 10^5$ | $F(1, 30) = 8.9$, $P = 0.006$ |
| 5.6 | $1.0 \times 10^6$ | $7.0 \times 10^5$ | $F(1, 30) = 8.6$, $P = 0.006$ |
| 11.2 | $5.7 \times 10^6$ | $7.6 \times 10^6$ | $F(1, 30) = 13.7$, $P = 0.001$ |

Data represent the low frequency component given genotype; male and female data are pooled. Data are expressed as mean ± S.D. The *p*-values are the results of main effects analysis.

female or male; therefore, we suggest recording mesopic-adapted fERGs and including sex as a variable in future fERG data analyses. Furthermore, we explored two additional dependent variables not examined by the schizophrenic-fERG literature to date, the b-/a-wave ratio and the-low frequency component of the Fourier transform analysis. Our work demonstrated that the b-/a-wave ratio did not depend on sex and can be used exclusively to evaluate genotypic differences. Finally, the low-frequency component of the fERG, which reflects the a- and b-waves combined, can inform about sex and genotype differences, as well, and it can be a better measure for recording in instances with a low

Investigative Ophthalmology & Visual Science

**Table 9.** Comparison of Low Frequency Component in WT and $SR^{-/-}$ Mice Depending on Sex

| Flash Intensity ($cd \cdot s/m^2$) | Female | | Male | | | Simple Main Effects | |
|---|---|---|---|---|---|---|---|
| | WT | $SR^{-/-}$ | WT | $SR^{-/-}$ | Interaction Sex*Genotype | Sex | Genotype |
| 0.175 | $4.5 \times 10^5$ | $6.2 \times 10^5$ | $6.4 \times 10^5$ | $2.9 \times 10^5$ | $F(1, 30) = 6.9, P = 0.013$ | Male: $P = 0.020$ | $SR^{-/-}$: $P = 0.023$ |
| 0.35 | $5.4 \times 10^5$ | $4.5 \times 10^5$ | $7.3 \times 10^5$ | $3.5 \times 10^5$ | $F(1, 30) = 4.7, P = 0.038$ | Male: $P < 0.0005$ | NS |
| 0.7 | $6.1 \times 10^5$ | $5.1 \times 10^5$ | $8.1 \times 10^5$ | $3.7 \times 10^5$ | $F(1, 30) = 5.3, P = 0.028$ | Male: $P < 0.0005$ | NS |
| 1.4 | $8.2 \times 10^5$ | $6.2 \times 10^5$ | $9.4 \times 10^5$ | $5.1 \times 10^5$ | $F(1, 30) = 1.2, P = 0.276$ | NA | NA |
| 2.8 | $8.6 \times 10^5$ | $7.2 \times 10^5$ | $1.0 \times 10^6$ | $5.6 \times 10^5$ | $F(1, 30) = 2.5, P = 0.124$ | NA | NA |
| 5.6 | $9.1 \times 10^5$ | $7.9 \times 10^5$ | $1.2 \times 10^6$ | $6.0 \times 10^5$ | $F(1, 30) = 3.5, P = 0.070$ | NA | NA |
| 11.2 | $1.2 \times 10^6$ | $9.0 \times 10^5$ | $1.3 \times 10^6$ | $6.0 \times 10^5$ | $F(1, 30) = 2.6, P = 0.118$ | NA | NA |

Data represent mean power of the low frequency component for each genotype. Data are expressed as mean of each genotype. The *p*-values are the results of main effects analysis. Simple main effects for sex (SME: Sex) and genotype (SME: Genotype) are in the last two columns with *p*-values Bonferroni-adjusted within each simple main effect.

signal-to-noise ratio. Due to its sensitivity to sex and genotype, the b-wave amplitude and implicit time from mesopic-adapted fERGs emerged as potential candidates for use as a schizophrenia biomarker.

Our negative results on the light- and dark-adapted fERGs were surprising, but they shed light on why there are inconsistent results in human studies. Recent ERG studies comparing subjects with schizophrenia to healthy human controls showed a reduction of the b-wave amplitude in subjects with schizophrenia under different light adaptation conditions.[2,3,12,13] Earlier work did not observe differences in fERG parameters in subjects with schizophrenia in comparison to controls.[63,64] The earlier and more recent studies differ in that the more recent analyses measured a variety of dependent variables in broader stimulus and background conditions. The reduced mesopic b-wave amplitude and delayed implicit times at all light intensities in $SR^{-/-}$ mice compared to WT mice agreed with these earlier studies in subjects with schizophrenia compared to healthy controls under their phototopic 1 (P1) condition.[2] Although a distinction between mesopic and light adaptation was not made in the study by Demmin et al.,[2] their results nonetheless shed light on the possibility of using mesopic adaptation to detect ERG abnormalities in subjects with schizophrenia. Unlike dark- and light-adapted fERGs, mesopic adaptation of fERGs encompasses a retinal network that integrates signals from both rods and cones. Studies have found that mesopic background light enhances and modulates the ERG photoresponse of the cones in a reversible manner,[65] possibly by decoupling the gap junctions between rods and cones that suppresses the cone ERG photoresponses during dark adaptation. This result implies that gap junctional coupling between rods and cones is modulated by background light, whereby mesopic lighting conditions decouple the gap junction, increasing the functional range of the cone light response.[65]

Aside from the initial gap junction connectivity between rods and cones, there are two other routes where these signals converge to include gap junctions; one of them is between AII amacrine cells and chemical synapses between on- and off-bipolar cells that are modulated by rods via a chemical synapse between rod bipolar cells and AII amacrine cells.[66] The diverse routes for rod–cone signaling imply that different retinal networks serve to transition from rod to cone vision across the range of mesopic light intensities. Although there is a rich body of literature describing the rod–cone pathways, the role that D-serine plays in these pathways has not been investigated. Our body of work suggests that D-serine plays a role in the rod–cone networks such that it impacts the on-bipolar response to the mesopic background. The ERG b-wave reflects primarily the activity of on-bipolar cells. We showed that D-serine was positively expressed in bipolar cells, and the significant decrease in D-serine levels from birth affected bipolar cell function during mesopic light conditions. This highlights the importance of examining mesopic-adapted fERGs in future studies and accounting for sex differences in analyses of electroretinographic measurements from people with schizophrenia.[49]

The b-/a-wave ratio has not been examined previously in the human fERG literature on subjects with schizophrenia nor in animal models of schizophrenia. It was reported to be a good marker for central retinal vein occlusion and predicting neovascular glaucoma.[67,68] Because the mesopic b-wave amplitude was significantly reduced in $SR^{-/-}$ mice but the a-wave amplitude was not, calculation of the b-/a-wave ratios allowed evaluation of its usefulness in quantifying genotypic differences. In the $SR^{-/-}$ NMDAR hypofunction mice, the b-/a-wave ratio was reduced at all light intensities in comparison to WT mice. This reduction was independent of the sex of the animal and therefore can be used as a tool to evaluate genotypic differences in b-wave parameters when data from both sexes are pooled together.

In addition to performing traditional quantification of the fERG a- and b-wave components, we implemented a higher order analysis on these components, the fast Fourier transform (FFT), even though analyses of the fERG waves using this technique have not been reported in human subjects with schizophrenia previously. In normal ERGs from human subjects, FFT measurements were better at reflecting differences than traditional amplitude and implicit time measurements because of their resistance to a low signal-to-noise variability.[69] We conducted frequency domain measurements due to their translational potential of reducing inherent variability brought about by the population studied.[69] In our work, the low-frequency component was significantly reduced in $SR^{-/-}$ NMDAR hypofunction mice in mesopic light adaptation in comparison to controls. Similar to the b-wave amplitude, the low-frequency component provides information on genotype and sex differences. In contrast to the b-wave amplitude, the low-frequency component also can account for inherent variability[69] in the data resulting from studying individuals with schizophrenia.[70] We suggest that an analysis of the low-frequency component

Investigative Ophthalmology & Visual Science

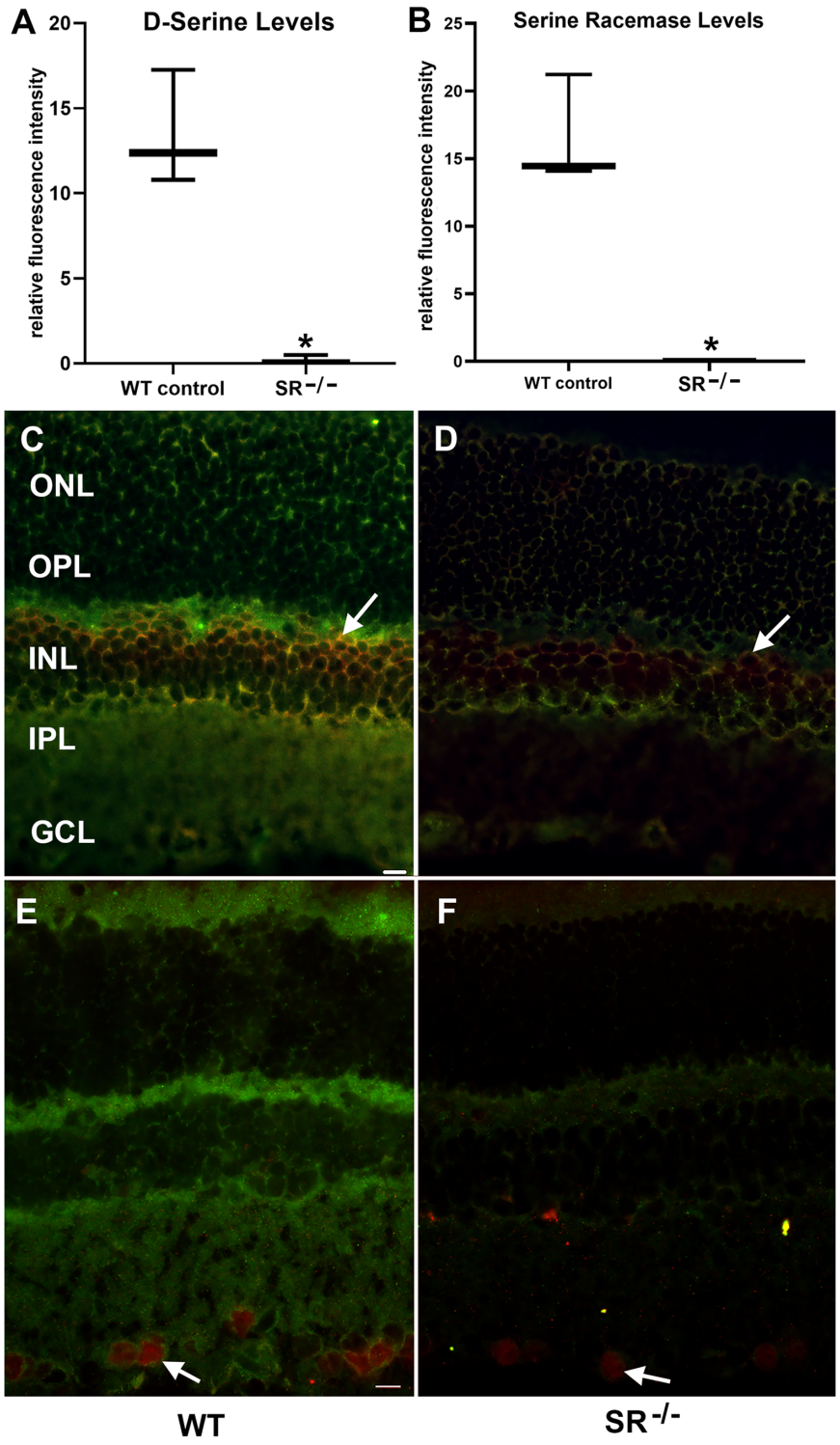


**Figure 7.** Densitometric and immunohistochemical examination of D-serine and serine racemase. Densitometric analysis demonstrated significant reduction of both D-serine levels (A) and serine racemase levels (B) in the *SR*$^{-/-}$ mice compared to littermate controls. Immunostaining demonstrated expression of D-serine at the highest levels in the inner nuclear layer (C, E), specifically in CHX10-positive bipolar cells (arrows, C, D), and in the inner plexiform and ganglion cell layers (C, E), specifically in brn3A-positive ganglion cells (arrows, E, F). Bar represents 10 µm. ONL, outer nuclear layer; OPL, outer plexiform layer; INL, inner nuclear layer; IPL, inner plexiform layer; GCL, ganglion cell layer.

Investigative Ophthalmology & Visual Science

be included in fERG analyses of people with schizophrenia to better differentiate their fERGs from those of control subjects.

Our research strongly supports the value of the $SR^{-/-}$ mouse model of schizophrenia, consistent with the NMDAR hypofunction hypothesis contributing to the pathophysiology of schizophrenia.[71] This mouse model would facilitate investigation into potential therapeutic interventions that might ameliorate these abnormalities in the retina and, by extension, within the brain. Previously tested mouse models with relevance to psychiatric disorders examined fERG changes resulting from dopaminergic dysfunction.[8] Lavoie and colleagues[8] observed a reduction in the b-wave amplitude at all light intensities in both photopic and scotopic conditions in dopamine D1 receptor knockout (D1R-KO) mice and commented on the similarity between D1R-KO results and high-risk schizophrenic offsprings. However, this reduction in b-wave was expected from knocking-out the D1 receptor, a dopamine receptor type known to be expressed in bipolar cells[72] and essential for normal response to light adaptation from bipolar cells.[73,74] Although other monoamine-deficient mice were examined and no significant differences were observed, the question now is whether there are any deficiencies in the fERGs of the mice tested by Lavoie et al.[8] during mesopic adaptation, specifically on the three dopamine transgenic mice tested, as dopamine is known to modulate the electrical coupling of the gap junction between rods and cones in the switch between photopic and mesopic lighting.[75]

The value of the $SR^{-/-}$ mouse is in explaining how D-serine is involved in shaping retinal network development and function. It has been shown that SR and D-serine expression normally changes dynamically in the retina with age, with D-serine being abundant earlier in development and declining in the first month of life.[76] In comparison to infant mice (3 weeks old), the adult mouse retina had limited D-serine and SR expression.[77] At present, it is not known why serine racemase and D-serine are so abundant early in development. The fact that we used a constitutively expressed mutation of SR, which would be true for subjects with the SR risk gene, may have impacted retinal development affected by NMDAR function. The onset of schizophrenia is not linked to the onset of psychosis, which typically occurs in the late teens or early 20s in males.[78] Cognitive impairments and social/motivational deficits (negative symptoms), which best reflect NMDAR hypofunction, are present in childhood in most individuals who later are diagnosed with schizophrenia after the appearance of psychosis.[79] Thus, this mouse model can show within-subject longitudinal differences due to SR and D-serine deprivation during development that may be relevant to changes associated with the onset of psychosis in schizophrenia.

Importantly, our study demonstrated distinctly different patterns of fERGs in male and female mice in mesopic-adapted fERGs, showing significant changes in the male $SR^{-/-}$ mice compared to WT mice but not in females. We did not see significant sex differences in light- and dark-adapted fERGs, which raises the question of the role of gonadal hormones in the transition between different background lights. Although some fERG studies in subjects with schizophrenia demonstrated that components of the photopic a- and b-waves were reduced in those with schizophrenia in comparison to healthy controls, most studies grouped male and female subjects for their data analyses. Only one study included sex as a factor, and they did not observe a statistically significant difference in fERGs between females and males with schizophrenia.[12] However, this study measured subjects that were at high risk for schizophrenia and did not account for sex in the follow-up study examining subjects who had developed schizophrenia.[7] It is difficult to interpret these results because questions remain as to the cause and effect of these relationships. There is little on sex differences in retinal function in the literature; however, some studies showed a sex difference in the fERGs among healthy human controls, including differences in amplitude and implicit time.[51,80] This is reflected in our work, whereby the mesopic fERGs of WT mice differed depending on sex at specific parameters. Previous studies have shown that the prevalence of schizophrenia is lower in females, who also have a later age of onset and a less severe disease course than males.[81–83] Notably, the behavioral phenotype was less severe in female $SR^{-/-}$ mice than in males.[15]

The power of the present study is twofold. First, we demonstrate that our current knowledge of the role D-serine in the retina requires further investigation due to the reduction of the mesopic b-wave amplitude and time delay observed in $SR^{-/-}$ mice. It is important to understand how the changes in D-serine and SR expression during development[76,84] reflect changes in the fERG at various light intensities and background conditions. D-Serine plays a pivotal role in the retina as the endogenous co-agonist of the NMDAR.[34] Because it is known that NMDARs are recruited in RGCs based on light intensity demands, looking at a range of light intensities can serve as an indirect evaluation of dynamic recruitment of NMDARs that may differentiate one person with schizophrenia from another.[85] As a result, we recommend evaluating a wider range of flash intensities under photopic, scotopic, and mesopic background adaptation to evaluate distinct retinal pathways in subjects with schizophrenia in comparison with controls.

Second, we demonstrated that signals from mesopic-adapted retina warrant further investigation regarding inner retinal involvement in the fERG,[86] particularly how these changes can be used as a potential diagnostic tool for identification of psychiatric disorders. Dopamine plays a role in switching between photopic and mesopic states.[75] This suggests that the network needed for adapting to mesopic light conditions can be severely affected by neuropsychiatric disorders such as schizophrenia, because it requires both dopamine and glutamate. It is the general consensus that schizophrenia is a disorder of complex genetics and that no single molecular event can account for the pathophysiology of schizophrenia,[85] which implies that people with schizophrenia may be quite diverse in the underlying cause of their disorder. This may explain the inconsistent results from human fERG data from people with schizophrenia.[2–4,6,7,61] Including mesopic-adapted conditions when studying human fERG responses may provide further insight. Our results demonstrate that specific analyses of the ERG waveform under a wider spectrum of background light conditions may allow more accurate and sensitive measures of differences between people with schizophrenia and normal individuals. The replication of the fERG results in individuals with schizophrenia using the methods used with this mouse model would further support the potential role of NMDAR hypofunction as one of the causative mechanisms. This mouse model will allow us to assess methods that might modify the abnormal fERGs that

Investigative Ophthalmology & Visual Science

may in turn result in new therapeutic approaches for the treatment of schizophrenia.

In conclusion, even though the current diagnostic measurement using clinical interviews is effective at identifying schizophrenia when psychosis is present, clinical screens prior to the appearance psychosis are only weakly predictive of schizophrenia.[10] The power of having a biomarker for schizophrenia risk lies on prognostics, the ability to predict who will become ill prior to the onset of psychosis. As there are known genetic risk factors for the development of schizophrenia,[87,88] this may aid in the early identification of at-risk individuals with impaired NMDAR function and thereby facilitate early intervention. The human studies demonstrate that there are anomalies in the fERGs of humans with schizophrenia in comparison to unaffected persons; however, insights into the cellular mechanisms behind these differences are needed. Further studies in this and other validated mouse models of schizophrenia should help explain why the fERG differences are present and provide stronger support for the use of fERGs as a tool to decipher the etiology of schizophrenia.

## *Acknowledgments*

Behavioral ERG testing was performed utilizing resources in the Mouse Behavior Core, University of Minnesota. We thank Dwight Burkhardt, PhD, for his critical reading of the manuscript and Heidi Röhrich for her excellent histological assistance.

Supported by National Institutes of Health Grants 1F31MH106296-01 (NTJ), 1F31AG057155-01A1 (JWL), R01 EY15313 (LKM), R21 EY025027 (RFM), T32 EY025187, and P30 EY11375; Office of the Vice President for Research (NTJ); and the Minnesota Lions Foundation.

Disclosure: **N. Torres Jimenez**, None; **J.W. Lines**, None; **R.B. Kueppers**, None; **P. Kofuji**, None; **H. Wei**, None; **A. Rankila**, None; **J.T. Coyle**, D-serine (P), Concert Pharma (C); **R.F. Miller**, None; **L.K. McLoon**, None

## *References*

1. London A, Benhar I, Schwartz M. The retina as a window to the brain-from eye research to CNS disorders. *Nat Rev Neurol*. 2013;9:44–53.
2. Demmin DL, Davis Q, Roche M, Silverstein SM. Electroretinographic anomalies in schizophrenia. *J Abnorm Psychol*. 2018;127:417–428.
3. Gerbaldo H, Thaker G, Tittel PG, Layne-Gedge J, Moran M, Demisch L. Abnormal electroretinography in schizophrenic patients with a history of sun gazing. *Neuropsychobiology*. 1992;25:99–101.
4. Raese JD, King RJ, Barnes D, Berger PA, Marmor MF, Hock P. Retinal oscillatory potentials in schizophrenia: implications for the assessment of dopamine transmission n man. *Psychopharmacol Bull*. 1982;18:72–78.
5. Warner R, Laugharne J, Peet M, Brown L, Rogers N. Retinal function as a marker for cell membrane omega-3 fatty acid depletion in schizophrenia: a pilot study. *Biol Psychiatry*. 1999;45:1138–1142.
6. Balogh Z, Benedek G, Keri S. Retinal dysfunctions in schizophrenia. *Prog Neuropsychopharmacol Biol Psychiatry*. 2008;32:297–300.
7. Hebert M, Merette C, Paccalet T, et al. Light evoked potentials measured by electroretinogram may tap into the neurodevelopmental roots of schizophrenia. *Schizophr Res*. 2015;162:294–295.
8. Lavoie J, Illiano P, Sotnikova TD, Gainetdinov RR, Beaulieu JM, Hebert M. The electroretinogram as a biomarker of central dopamine and serotonin: potential relevance to psychiatric disorders. *Biol Psychiatry*. 2014;75:479–486.
9. Nguyen CTO, Hui F, Charng J, et al. Retinal biomarkers provide "insight" into cortical pharmacology and disease. *Pharmacol Ther*. 2017;175:151–177.
10. Weickert CS, Weickert TW, Pillai A, Buckley PF. Biomarkers in schizophrenia: a brief conceptual consideration. *Dis Markers*. 2013;35;3–9
11. Savill M, D'Ambrosio J, Cannon TD, Loewy RL. Psychosis risk screening in different populations using the Prodromal Questionnaire: a systematic review. *Early Interv Psychiatry*. 2018;12:3–14.
12. Hebert M, Gagne AM, Paradis ME, et al. Retinal response to light in young nonaffected offspring at high genetic risk of neuropsychiatric brain disorders. *Biol Psychiatry*. 2010;67:270–274.
13. Granit R. The components of the retinal action potential in mammals and their relation to the discharge in the optic nerve. *J Physiol*. 1933;77:207–239.
14. Frishman L, Wang MN. Electroretinogram of human, monkey and mouse. *Adler's Physiology of the Eye*. 11th Edition. Edinburgh: Saunders; 2010:480–501.
15. Föcking M, Lopez LM, English JA, *et al*. Proteomic and genomic evidence implicates the postsynaptic density in schizophrenia. *Mol Psychiatry*. 2015;20:424–432.
16. Tomasetti C, Iasevoli F, Buonaguro EF, et al. Treating the synapse in major psychiatric disorders: the role of postsynaptic density network in dopamine-glutamate interplay and psychopharmacologic drugs molecular action. *Int J Mol Sci*. 2017;18:135.
17. Balu DT, Coyle JT. The NMDA receptor 'glycine modulatory site' in schizophrenia: D-serine, glycine, and beyond. *Curr Opin Pharmacol*. 2015;20:109–115.
18. Basu AC, Tsai GE, Ma CL, et al. Targeted disruption of serine racemase affects glutamatergic neurotransmission and behavior. *Mol Psychiatry*. 2009;14:719–727.
19. Dizon DB, Copenhagen DR. Two types of glutamate receptors differentially excite amacrine cells in the tiger salamander retina. *J Physiol*. 1992;449:589–606.
20. Haverkamp S, Wassle H. Immunocytochemical analysis of the mouse retina. *J Comp Neurol*. 2000;424:1–23.
21. Mittman S, Taylor WR, Copenhagen DR. Concomitant activation of two types of glutamate receptor mediates excitation of salamander retinal ganglion cells. *J Physiol*. 1990;428:175–197.
22. Luby ED, Gottlieb JS, Cohen BD, Rosenbaum G, Domino EF. Model psychoses and schizophrenia. *Am J Psychiatry*. 1962;119:61–67.
23. Goff DC, Tsai G, Manoach DS, Coyle JT. Dose-finding trial of D-cycloserine added to neuroleptics for negative symptoms in schizophrenia. *Am J Psychiatry*. 1995;152:1213–1215.
24. Goff DC, Tsai G, Levitt J, et al. A placebo-controlled trial of D-cycloserine added to conventional neuroleptics in patients with schizophrenia. *Arch Gen Psychiatry*. 1999;56:21–27.
25. Chumakov I, Blumenfeld M, Guerassimenko O, et al. Genetic and physiological data implicating the new human gene G72 and the gene for D-amino acid oxidase in schizophrenia. *Proc Natl Acad Sci USA*. 2002;99:13675–13680.
26. Yamada K, Ohnishi T, Hashimoto K, et al. Identification of multiple serine racemase (SRR) mRNA isoforms and genetic analyses of SRR and DAO in schizophrenia and D-serine levels. *Biol Psychiatry*. 2005;57:1493–1503.

27. Yurgelun-Todd DA, Coyle JT, Gruber SA, et al. Functional magnetic resonance imaging studies of schizophrenic patients during word production: effects of D-cycloserine. *Psychiatry Res*. 2005;138:23–31.
28. Leiderman E, Zylberman I, Zukin SR, Cooper TB, Javitt DC. Preliminary investigation of high-dose oral glycine on serum levels and negative symptoms in schizophrenia: an open-label trial. *Biol Psychiatry*. 1996;39:213–215.
29. Tsai G, Passani LA, Slusher BS, et al. Abnormal excitatory neurotransmitter metabolism in schizophrenic brains. *Arch Gen Psychiatry*. 1995;52:829–836.
30. Weickert CS, Fung SJ, Catts VS, et al. Molecular evidence of *N*-methyl-D-aspartate receptor hypofunction in schizophrenia. *Mol Psychiatry*. 2013;18:1185–1192.
31. Hashimoto K, Engberg G, Shimizu E, Nordin C, Lindstrom LH, Iyo M. Reduced D-serine to total serine ratio in the cerebrospinal fluid of drug naive schizophrenic patients. *Prog Neuropsychopharmacol Biol Psychiatry*. 2005;29:767–769.
32. Javitt DC, Zukin SR. Recent advances in the phencyclidine model of schizophrenia. *Am J Psychiatry*. 1991;148:1301–1308.
33. Labrie V, Fukumura R, Rastogi A, et al. Serine racemase is associated with schizophrenia susceptibility in humans and in a mouse model. *Hum Mol Genet*. 2009;18:3227–3243.
34. Stevens ER, Gustafson EC, Sullivan SJ, Esguerra M, Miller RF. Light-evoked NMDA receptor-mediated currents are reduced by blocking D-serine synthesis in the salamander retina. *Neuroreport*. 2010;21:239–244.
35. Blokhuis C, Demirkaya N, Cohen S, et al. The eye as a window to the brain: neuroretinal thickness is associated with microstructural white matter injury in HIV-infected children. *Invest Ophthalmol Vis Sci*. 2016;57:3864–3871.
36. Chu EMY, Kolappan M, Barnes TRE, Joyce EM, Ron MA. A window into the brain: an in vivo study of the retina in schizophrenia using optical coherence tomography. *Psychiat Res*. 2012;203:89–94.
37. Schönfeldt-Lecuona C, Kregel T, Schmidt A, et al. From imaging the brain to imaging the retina: optical coherence tomography (OCT) in schizophrenia. *Schizophr Bull*. 2016;42:9–14.
38. Silverstein SM, Rosen R. Schizophrenia and the eye. *Schizophr Res Cogn*. 2015;2:46–55.
39. Lavoie J, Aziade M, Hebert M. The brain through the retina: the flash electroretinogram as a tool to investigate psychiatric disorders. *Prog Neuropsychopharmacol Biol Psychiatry*. 2014;48:129–134.
40. Brown KT, Wiesel TN. Localization of origins of electroretinogram components by intraretinal recording in the intact cat eye. *J Physiol*. 1961;158:257–280.
41. Penn RD, Hagins WA. Kinetics of the photocurrent of retinal rods. *Biophys J*. 1972;12:1073–1094.
42. Penn RD, Hagins WA. Signal transmission along retinal rods and the origin of the electroretinographic a-wave. *Nature*. 1969;223:201–204.
43. Robson JG, Frishman LJ. Response linearity and kinetics of the cat retina: the bipolar cell component of the dark-adapted electroretinogram. *Vis Neurosci*. 1995;12:837–850.
44. Stockton RA, Slaughter MM. B-wave of the electroretinogram. A reflection of ON bipolar cell activity. *J Gen Physiol*. 1989;93:101–122.
45. Miura G, Wang MH, Ivers KM, Frishman LJ. Retinal pathway origins of the pattern ERG of the mouse. *Exp Eye Res*. 2009;89:49–62.
46. Kinoshita J, Peachey NS. Noninvasive electroretinographic procedures for the study of the mouse retina. *Curr Protoc Mouse Biol*. 2018;8:1–6.
47. Kofuji P, Ceelen P, Zahs KR, Surbeck LW, Lester HA, Newman EA. Genetic inactivation of an inwardly rectifying potassium channel (Kir4.1 subunit) in mice: phenotypic impact in retina. *J Neurosci*. 2000;20:5733–5740.
48. Wachtmeister L. Oscillatory potentials in the retina: what do they reveal. *Prog Retin Eye Res*. 1998;17:485–521.
49. Zeidler I. The clinical electroretinogram: IX. The normal electroretinogram. IX: Value of the b-potential in different age groups and its differences in men and women. *Acta Ophthalmol (Copenh)*. 1959;37:294–301.
50. Vainio-Mattila B. The clinical electroretinogram: II. The difference between the electroretinogram in men and in women. *Acta Ophthalmol (Copenh)*. 1951;29:25–32.
51. Peterson H. The normal B-potential in the single-flash clinical retinogram. A computer technique study of the influence of sex and age. *Acta Ophthalmol (Copenh)*. 1968;99(Suppl):7–77.
52. Faraone SV, Chen WJ, Goldstein JM, Tsuang MT. Gender differences in age at onset of schizophrenia. *Br J Psychiatry*. 1994;164:625–629.
53. Hafner H. Gender differences in schizophrenia. *Psychoneuroendocrinology*. 2003;28(Suppl 2):17–54.
54. Ochoa S, Usall J, Cobo J, Labad X, Kulkarni J. Gender differences in schizophrenia and first-episode psychosis: a comprehensive literature review. *Schizophr Res Treatment*. 2012;2012:916198.
55. McCulloch DL, Marmor MF, Brigell MG, et al. ISCEV standard for full-field clinical electroretinography (2015 update). *Doc Ophthalmol*. 2015;130:1–12.
56. Bresnick GH, Palta M. Temporal aspects of the electroretinogram in diabetic retinopathy. *Arch Ophthalmol*. 1987;105:660–664.
57. Tahara K, Matsuura T, Otori T. Diagnostic evaluation of diabetic retinopathy by 30-Hz flicker electroretinography. *Jpn J Ophthalmol*. 1993;37:204–210.
58. Anis NA, Berry SC, Burton NR, Lodge D. The dissociative anaesthetics, ketamine and phencyclidine, selectively reduce excitation of central mammalian neurones by *N*-methyl-aspartate. *Br J Pharmacol*. 1983;79:565–575.
59. Woodward WR, Choi D, Grose J, et al. Isoflurane is an effective alternative to ketamine/xylazine/acepromazine as an anesthetic agent for the mouse electroretinogram. *Doc Ophthalmol*. 2007;115:187–201.
60. Asi H, Perlman I. Relationships between the electroretinogram a-wave, b-wave and oscillatory potentials and their application to clinical diagnosis. *Doc Ophthalmol*. 1992;79:125–139.
61. Benchorin G, Calton MA, Beaulieu MO, Vollrath D. Assessment of murine retinal function by electroretinography. *Bio Protoc*. 2017;7:e2218.
62. Sullivan SJ, Esquerra M, Wickham RJ, Romero GE, Coyle JT, Miller RF. Serine racemase deletion abolishes light-evoked NMDA receptor currents in retinal ganglion cells. *J Physiol*. 2011;589:5997–6006.
63. Schechter G, Hock P, Rodgers K, Pfefferbaum A, Marmor MF, Berger PA. Electroretinographic assessment in schizophrenia. *Electroencephalogr Clin Neurophysiol Suppl*. 1987;40:746–751.
64. Marmor MR, Hock P, Schechter G, Pfefferbaum A, Berger PA, Maurice R. Oscillatory potentials as a marker for dopaminergic disease. *Doc Ophthalmol*. 1988;69:255–261.
65. Heikkinen H, Vinberg F, Nymark S, Koskelainen A. Mesopic background lights enhance dark-adapted cone ERG flash responses in the intact mouse retina: a possible role for gap junctional coupling. *J Neurophysiol*. 2011;105:2309–2318.
66. Grimes WN, Songo-Aguas A, Rieke F. Parallel processing of rod and cone signals: retinal function and human perception. *Annu Rev Vis Sci*. 2018;4:123–141.


Investigative Ophthalmology & Visual Science

67. Sabates R, Hirose T, McMeel JW. Electroretinography in the prognosis and classification of central retinal vein occlusion. *Arch Ophthalmol*. 1983;101:232–235.
68. Matsui Y, Katsumi O, Sakaue H, Hirose T. Electroretinogram b/a wave ratio improvement in central retinal vein obstruction. *Br J Ophthalmol*. 1994;78:191–198.
69. Gur M, Zeevi Y. Frequency-domain analysis of the human electroretinogram. *J Opt Soc Am*. 1980;70:53–59.
70. Moghimi P, Torres Jimenez N, McLoon LK, et al. Electoretinographic evidence of retinal ganglion cell-dependent function in schizophrenia. *Schizophr Res*. 2019. doi:10.1016/j.schres.2019.09.005. [Epub ahead of print].
71. APA. *Diagnostic and Statistical Manual of Mental Disorders*. 5th Edition. Arlington, VA: American Psychiatric Association; 2013.
72. Farshi P, Fyk-Kolodziej B, Krolewski DM, Walker PD, Ichinose T. Dopamine D1 receptor expression is bipolar cell type-specific in the mouse retina. *J Comp Neurol*. 2016;524:2059–2079.
73. Chen S, Zhi ZN, Ruan QQ, et al. Bright light suppresses form-deprivation myopia development with activation of dopamine D1 receptor signaling in the ON pathway in retina. *Invest Ophthalmol Vis Sci*. 2017;58:2306–2316.
74. Flood MD, Moore-Dotson JM, Eggers ED. Dopamine D1 receptor activation contributes to light-adapted changes in retinal inhibition to rod bipolar cells. *J Neurophysiol*. 2018;120:867–879.
75. Krizaj D. Mesopic state: cellular mechanisms involved in pre- and post-synaptic mixing of rod and cone signals. *Microsc Res Tech*. 2000;50:347–359.
76. Romero GE, Lockridge AD, Morgans CW, Bandyopadhyay D, Miller RF. The postnatal development of D-serine in the retinas of two mouse strains, including a mutant mouse with a deficiency in D-amino oxidase and a serine racemase knockout mouse. *ACT Chem Neurosci*. 2014;5:848–854.
77. Dun Y, Duplantier J, Roon P, Martin PM, Ganapathy V, Smith SB. Serine racemase expression and D-serine content are developmentally regulated in neuronal ganglion cells of the retina. *J Neurochem*. 2008;104:970–978.
78. Hambrecht M, Maurer K, Hafner H, Sartorius N. Transnational stability of gender differences in schizophrenia? An analysis based on the WHO study on determinants of outcome of severe mental disorders. *Eur Arch Psychiatry Clin Neurosci*. 1992;242:6–12.
79. Loebel AD, Lieberman JA, Alvir JM, Mayerhoff DI, Geisler SH, Szymanski SR. Duration of psychosis and outcome in first-episode schizophrenia. *Am J Psychiatry*. 1992;149:1183–1189.
80. Brûlé J, Lavoie MP, Casanova C, Lachapelle P, Hebert M. Evidence of a possible impact of the menstrual cycle on the reproducibility of scotopic ERGs in women. *Doc Ophthalmol*. 2007;114:135–134.
81. Sannita WG, Maggi L, Germini PL, Fioretto M. Correlation with age and sex of flash-evoked electroretinogram and retinal oscillatory potentials recorded with skin electrodes. *Doc Ophthalmol*. 1989;71:413–419.
82. Loranger AW. Sex difference in age at onset of schizophrenia. *Arch Gen Psychiatry*. 1984;41:157–161.
83. Shepherd M, Watt D, Falloon I, Smeeton N. The natural history of schizophrenia: a five-year follow-up study of outcome and prediction in a representative sample of schizophrenics. *Psychol Med Monogr Suppl*. 1989;15:1–46.
84. Gustafson EC, Stevens ER, Wolosker H, Miller RF. Endogenous D-serine contributes to NMDA-receptor-mediated light-evoked responses in the vertebrate retina. *J Neurophysiol*. 2007;98:122–130.
85. Coyle JT. Glutamate and schizophrenia: beyond the dopamine hypothesis. *Cell Mol Neurobiol*. 2006;26:365–384.
86. Mojumder DK, Sherry DM, Frishman LJ. Contribution of voltage-gated sodium channels to the b-wave of the mammalian flash electroretinogram. *J Physiol*. 2008;586:2551–2560.
87. Baron M, Gruen R, Asnis L, Kane J. Age-of-onset in schizophrenia and schizotypal disorders. Clinical and genetic implications. *Neuropsychobiology*. 1983;10:199–204.
88. Kendler KS, Robinette CD. Schizophrenia in the National Academy of Sciences-National Research Council Twin Registry: a 16-year update. *Am J Psychiatry*. 1983;140:1551–1563.